A Compact Sagnac Loop Based on a Microfiber Coupler for Twist Sensing

Ye Chen, Yuliya Semenova, Gerald Farrell, Fei Xu, and Yan-Qing Lu

***Abstract*— We present a compact highly sensitive microfiber coupler-based twist sensor formed by fusing and tapering two optical fibers and then connecting two of the pigtails to form a Sagnac loop. The device is miniature, low cost, and easily fabricated. The sensor has high twist sensitivities of ∼0.9 nm/° when measuring wavelength shift and ∼0.16 dB/° when measuring transmission power, both of which confirm that the sensor has good potential for application in the structural health monitoring and other areas.**

***Index Terms*— Twist sensor, microfiber coupler, Sagnac loop.**

I. Introduction

TWIST sensing is of great importance in health monitoring of bridges, buildings, high-speed rails, etc. Traditional twist sensors based on electric or magnetic effects tend to be large in size and are susceptible to electromagnetic interference, which limit their uses [1].

Optical fiber twist sensors (OFTSs) are ideally suited to this application because of many desirable properties such as flexibility, ease of integration, multiplexing capability and a strong resistance to environmental interference, especially immunity to electromagnetic interference. Various types of twist angle sensors based on optical fibers have been demonstrated: OFTSs based on birefringent fibers [2], tilted fiber gratings (TFGs) [3], fiber Bragg gratings (FBGs) [4], [5], long-period fiber gratings (LPFGs) [6], photonic-crystal-fibers (PCFs) [7] and multi-mode interferometers (MMIs) [8]. Yet there remain several obstacles to wide usage for these sensors: gratings present strong cross sensitivity between strain and temperature, whereas the PCFs are costly, and the MMIs usually have complex fabrication techniques. Thus more effort is still required to demonstrate miniature, low cost and easily fabricated OFTSs.

Since the first report of the microfiber coupler (MFC) in 2009 [9], several MFC based devices with good performance have been demonstrated [10]–[12]. A typical MFC is fabricated from two commercial fibers (SMF 28) using a flame-brushing technique [13]. The material promises a low cost and the fabrication method is quite simple. In this letter, we present a highly sensitive OFTS based on MFC. The sensitivity of the birefringence caused envelope peak wavelength is ∼0.9 nm/degree and the sensitivity of coupling peak power is ∼0.16 dB/degree, showing better performances than former reports [2]–[4], [14].

Manuscript received July 27, 2015; revised September 8, 2015; accepted September 9, 2015. Date of publication September 18, 2015; date of current version October 8, 2015. This work was supported in part by the Science Foundation Ireland (SFI) through the International Strategic Cooperation Award under Grant SFI/13/ISCA/2845, in part by the China National 973 Program under Grant 2012CB921803 and Grant 2011CBA00205, and in part by the National Natural Science Foundation of China under Grant 61322503 and Grant 61475069.

Y. Chen is with the National Laboratory of Solid State Microstructures, College of Engineering and Applied Sciences, Nanjing University, Nanjing 210093, China, and also with the Photonics Research Center, Dublin Institute of Technology, Dublin 8, Ireland (e-mail: yechennju@gmail.com).

Y. Semenova and G. Farrell are with the Photonics Research Center, Dublin Institute of Technology, Dublin 8, Ireland (e-mail: yuliya.semenova@dit.ie; gerald.farrell@dit.ie).

F. Xu and Y.-Q. Lu are with the National Laboratory of Solid State Microstructures, College of Engineering and Applied Sciences, Nanjing University, Nanjing 210093, China (e-mail: feixu@nju.edu.cn; yqlu@nju.edu.cn).

Color versions of one or more of the figures in this letter are available online at http://ieeexplore.ieee.org.

Digital Object Identifier 10.1109/LPT.2015.2478479

II. Device Fabrication

Fig. 1(a) illustrates the schematic of our device. We first fabricated a MFC by laterally fusing and tapering two optical fibers. Then the two output ports were fused together to form a Sagnac loop. Taking the advantage of the birefringence in the coupling region, we reuse this region as the effective sensing region, making the device more compact than a system containing two separate devices.

The birefringence of the coupling region originates from its asymmetric structure [15], [16]. As we can see from Fig. 1(b), the shape of the waist cross section changes throughout the stretching process. In the first stage, the geometry can be assumed as two side-by-side touching cylinders, and thus we can analyze the output light and birefringence using weakly coupled model [17], in which the coupling coefficients for the x and y polarizations are given by:

$$\kappa_x = \frac{2^{2/3}(n_1^2 - n_0^2)^{1/2} U_\infty^2 (2n_1^2 V + 1)}{n_1^3 a(\sqrt{\pi}) V^{7/2}} \tag{1}$$

$$\kappa_y = \frac{2^{2/3}(n_1^2 - n_0^2)^{1/2} U_\infty^2 (2n_1^2 V - 1)}{n_1^3 a(\sqrt{\pi}) V^{7/2}} \tag{2}$$

where n_1 and n_0 are the refractive indices of silica and air, a is the diameter of one of the microfibers, and $U_\infty = 2.405$ and $V = [(2\pi a)/\lambda](n_1^2 - n_0^2)^{1/2}$. The normalized power at P_2 can be calculated as:

$$P_2 = \frac{1}{2}\{1 + \cos[2(\overline{\kappa_x} + \overline{\kappa_y})L_{coupler}]\cos[2(\overline{\kappa_x} - \overline{\kappa_y})L_{coupler}]\} \tag{3}$$

where $L_{coupler}$ is the coupling length of the MFC. $\overline{\kappa_x}$ and $\overline{\kappa_y}$ are the values of (1) and (2) averaged over the whole coupling region.

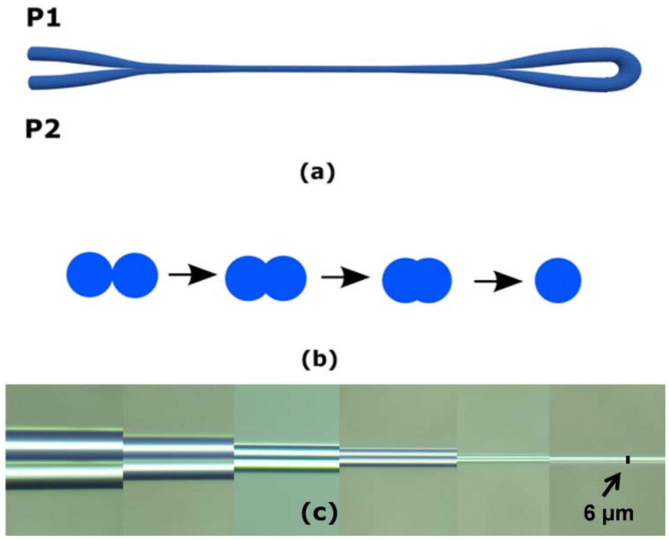

Fig. 1. (a) Diagram of the MFC based OFTS. (b) The shapes of the waist cross section of the MFC at different stages of the stretching process. (c) Microscope images of the MFC. The final section of the right side is the waist region. Each of the microfibers has a diameter ~3 μm. The waist region length is ~1.5 cm.

From (3) we can conclude that the output spectrum will show a slow modulation envelope which comes from $\cos[2(\overline{\kappa_x}-\overline{\kappa_y})L_{coupler}]$. Considering (1), (2) and the definition of V, we will find that the thinner the fiber is the higher is the birefringence, meaning a lager difference between κ_x and κ_y. As the stretching process continues, the well fused waveguide is better modeled by an equivalent rectangular waveguide [17]. The shape of the waist cross section finally becomes close to cylindrical under the influence of surface tension of the fused silica, which in turn results in a gradually decreasing birefringence. Above all, the birefringence first rises and then drops during the stretching process.

The key to achieving high twist sensitivity is finding the optimal MFC waist region parameters resulting in a suitable birefringence. In our experiment, the fabrication process of the MFC with optimal parameters is reproducible with the aid of the well-established flame brushing method. This method will provide a precise control of the coupler diameter and waist region length. In additional to the fabrication system, we also use an OSA for in situ monitoring to help us find the optimal MFC parameters.

Fig. 1(c) shows the microscope images of the MFC before twisting. The final section of the right side is the waist region, which has a length ~1.5 cm and diameter ~3 μm of each microfiber. This waist part of the MFC is the main twist region.

The sensing principle is determined by (3), which indicates the output power of the sensor. From this formula, we will find the envelope is determined by $\cos[2(\overline{\kappa_x}-\overline{\kappa_y})L_{coupler}]$ and the coupling peak relates to $\cos[2(\overline{\kappa_x}+\overline{\kappa_y})L_{coupler}]$. When there is a twist applied on the waist region, the shear strain will induce a circular birefringence while the device also has an intrinsic linear birefringence. It results in a general elliptical birefringence inside the coupling region. Twist caused birefringence change will then lead to a variation of $\kappa_x - \kappa_y$ while $\kappa_x + \kappa_y$ is not largely influenced, and the $L_{coupler}$ is quite constant during the experiment. Thus, we will find the coupling peak wavelength to be stable, while the peak power and envelope are changing along the twist process. In addition, since the twist, birefringence is determined by the twist rate, i.e. rotated induced angle per unit length, twist angle sensitivity also relates to the whole sensing region length. In our experiment, the device has a sensing length about ~1.5 cm.

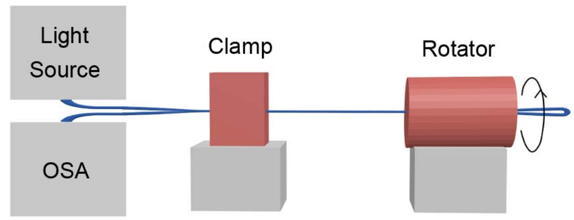

Fig. 2. Experiment setup for characterizing the OFTS.

III. Experiment and Analysis

The experimental setup for the characterization the OFTS is depicted in Fig. 2. The light from a broadband source (NKT Photonics) was launched into the input port P_1, and the output light from port P_2 was collected by the optical spectrum analyzer (AQ6317C, Yokogawa, Japan). The input and output pigtails of the MFC were fixed by a clamp and the Sagnac loop was fixed to a rotator. The fiber length between the clamp and rotator was ~6 cm. However, the effective sensing length is the coupling region, which is about ~1.5 cm. That is because the coupling region has a much thinner diameter than the pigtails, thus it is more flexible and easier to be twisted. What's more, there is no loss introduced by the clamp, as the clamp is only used to fix two pigtails, which are 125 μm-diameter fibers with protection coating.

Then, twist was applied in a step like fashion on the MFC in the clockwise direction from 0° to 80° using a rotator. During the experiment, we use the clamp to fix the pigtails and make sure the coupling region is straightly set up in the air. More protection can be done by coating the microfiber coupler by low refractive index polymer and package it inside the detected axletree.

Fig. 3 shows the SEM pictures of left, centre, and right parts of the MFC waist region after twisting. Each of the microfibers has a diameter ~3 μm. The coupling region is twist ~80 degree. From each picture, it is hard to find twist effect because the overall twist angle is ~80 degree along 1.5cm, which means less than 0.53 degree along several tens micrometers. By comparing the figures of three different parts of the waist region, we can still find out the twist caused structure change.

The transmission spectrum for each applied twist angle was recorded as shown in Fig. 4. In order to get the envelope, a fitting process was done by the following two steps: 1, find out the lower peak values (ignore the small dips); 2, interpolation to form a smooth curve. As we can see from Fig. 4(a), the envelope peak redshifts, and from Fig. 4(b) the power

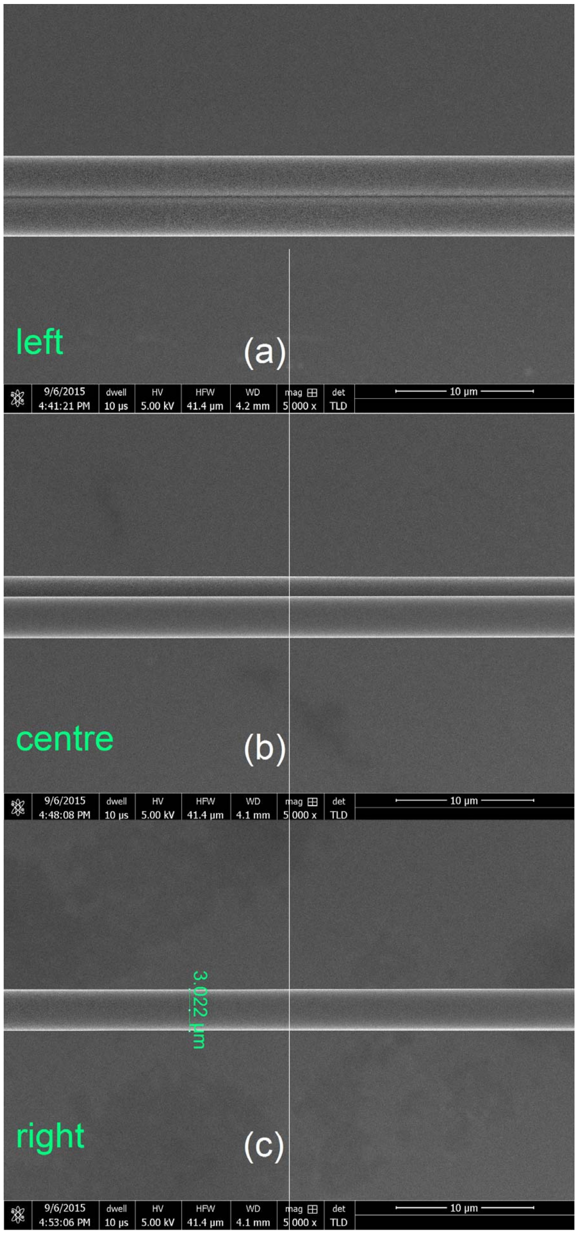

Fig. 3. SEM images of the (a) left, (b) centre, and (c) right parts of the MFC waist region. Each of the microfibers has a diameter $\sim$3 μm. The overall twist angle is $\sim$80 degree.

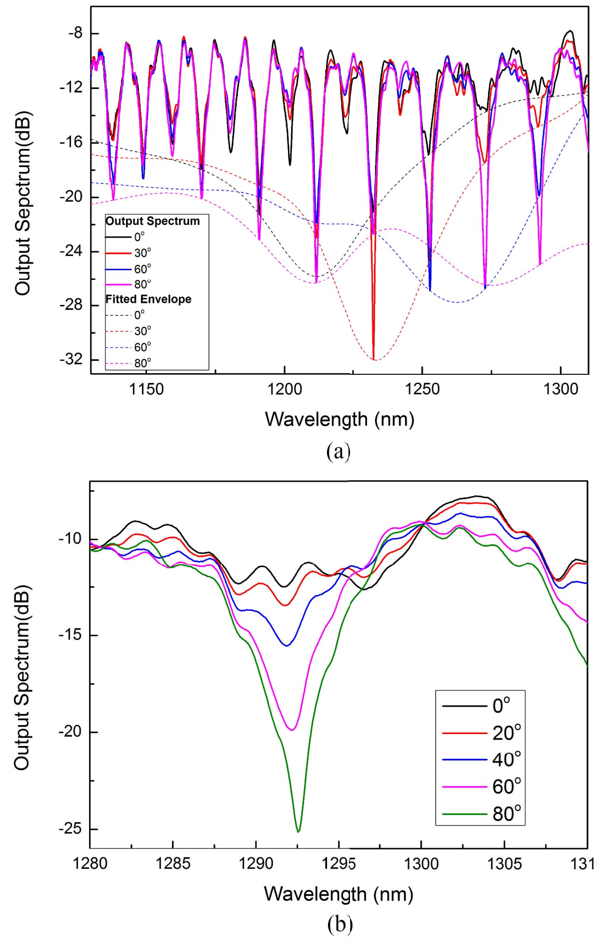

Fig. 4. (a) The solid lines are the output spectra and the dash dot lines are the fitted envelope curves. As the twist angle increases, the envelope peak redshifts; (b) the interference peak power around 1300nm decreases with the twist angle.

of interference peak around 1300 nm decreases. The small dips might come from the twist induced xy polarization mode coupling or higher order mode coupling, the envelope of the small dips is also influenced by the twist, it shows a blue shift and the dip power changes along. However, the effect is very weak. We do not take it into consideration here. The experimental results show that sensing of twist angle can be carried out either by measuring the envelope peak shift or by determining the twist angle from measurements of the peak power changes for a selected spectral peak.

Fig. 5(a) shows the results when the measurement of twist angle is carried out using envelope peak shifts. The peak wavelength moves form 1208.5 nm to 1279 nm. The resulting sensitivity is $\sim$0.9 nm/degree, which is higher than that of the previously reported fiber-based twist sensors [2].

Fig. 5(b) shows the experimental results if the measurement of twist angle is carried out using transmission power changes. The peak power around 1300 nm decreases from -12.7 dB to -25.2 dB with an average sensitivity about 0.16 dB/degree, which is better than the previously reported twist sensors based on fiber gratings [3], [4]. Reference [4] reported a twist sensor of which the sensitivity is 0.955 dB/rad and the sensing region length is about 1 cm, which is 0.167 dB/degree$\cdot$cm^{-1}. The device we present has a sensitivity $\sim$0.16 dB/degree over 1.5 cm, meaning 0.24 dB/degree$\cdot$cm^{-1}, which is slightly larger.

The detection range of our device is about $\pm$ 80 degree. For the envelope wavelength shift sensing method, the distance between two adjacent envelope peaks will limits the maximum twist angle. In order to increase the sensing range, we can enlarge this distance by decreasing the inherent birefringence of the coupling region. However, it will cause some disadvantages such as the FWHM broaden of envelope peak. Therefore, careful adjustment is needed to find a suitable parameter. For the transmission power measuring method, the maximum peak depth limits the twist angle. In order to increase the measurement range, we can raise the coupling efficiency by optimizing the fabrication processing. The counter-clockwise

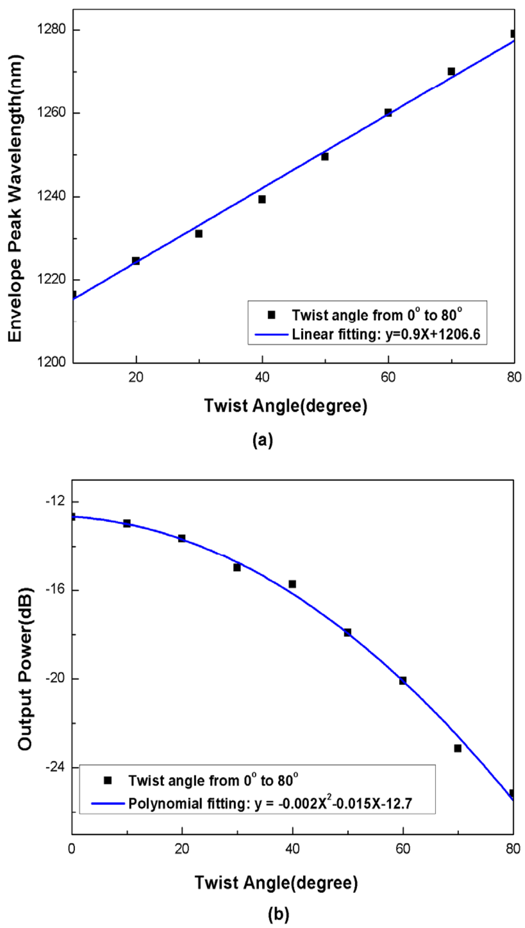

Fig. 5. (a) Envelope peak shift against twist angle; (b) peak power change around 1300 nm against twist angle.

rotation can also be detected, it will show a reverse process.

The coupling peak wavelength temperature sensitivity of our devices is ∼10 pm/°c, with a cross-sensitivity of ∼0.01 degree. It is the main issue of the detect limit. Further improvement will offer better stability by coating it with low refractive index and negative thermal-optical coefficient polymer or make use of the rich output information to separate the temperature and twist angle. Compared with other twist sensors, there are several advantages to use MFCs such as simple, easily fabricated, low cost and multiport structure.

IV. Conclusions

In this letter, we have demonstrated a miniature highly-sensitive Sagnac loop interferometer twist sensor based on a microfiber coupler. The Sagnac loop interferometer is formed by fusing and tapering two optical fibers and then connecting two of the pigtails. The sensor offers a range of advantages, such as compact size, low cost and ease of fabrication. The sensor has high twist sensitivities of circa 0.9 nm/degree by measuring wavelength shift and about 0.16 dB/degree by measuring transmission power which promises that the sensor has good potential for applications such as health monitoring of bridges, buildings, high-speed rails and other structural health monitoring situations.

Acknowledgment

The authors acknowledge Shao-cheng. C. Yan, W.ei Luo, and Q.i Wu for their kind help.

References

[1] V. Lemarquand, “Synthesis study of magnetic torque sensors,” *IEEE Trans. Magn.*, vol. 35, no. 36, pp. 4503–4510, Nov. 1999.
[2] H. Liang, Y. Jin, Y. Zhao, and J. Wang, “Twist sensor by using a pressure-induced birefringence single mode fiber based Sagnac interferometer,” in *Proc. ACP Asia*, Shanghai, China, 2011, pp. 1–6.
[3] Z. Yan, A. Adebayo, K. Zhou, L. Zhang, and D. Webb, “All-fibre twist sensor system based on 45° and 81° tilted fibre gratings,” *Proc. SPIE*, vol. 7753, p. 77538E, May 2011.
[4] Y. Wang, M. Wang, and X. Huang, “In fiber Bragg grating twist sensor based on analysis of polarization dependent loss,” *Opt. Exp.*, vol. 21, pp. 11913–11920, May 2013.
[5] J. H. Wo *et al.*, “Twist sensor based on axial strain insensitive distributed Bragg reflector fiber laser,” *Opt. Exp.*, vol. 20, pp. 2844–2850, Jan. 2012.
[6] J. Y. Cho, J. H. Lim, and K. S. Lee, “Optical fiber twist sensor with two orthogonally oriented mechanically induced long-period grating sections,” *IEEE Photon. Technol. Lett.*, vol. 17, no. 2, pp. 453–455, Feb. 2005.
[7] H.-M. Kim, T.-H. Kim, B. Kim, and Y. Chung, “Temperature-insensitive torsion sensor with enhanced sensitivity by use of a highly birefringent photonic crystal fiber,” *IEEE Photon. Technol. Lett.*, vol. 22, no. 20, pp. 1539–1541, Oct. 15, 2010.
[8] B. Song, Y. Miao, W. Lin, H. Zhang, J. Wu, and B. Liu, “Multi-mode interferometer-based twist sensor with low temperature sensitivity employing square coreless fibers,” *Opt. Exp.*, vol. 21, pp. 26806–26811, Nov. 2013.
[9] Y. Jung, G. Brambilla, and D. J. Richardson, “Optical microfiber coupler for broadband single-mode operation,” *Opt. Exp.*, vol. 17, pp. 5273–5278, Mar. 2009.
[10] Y. Jung *et al.*, “Dual mode fused optical fiber couplers suitable for mode division multiplexed transmission,” *Opt. Exp.*, vol. 21, pp. 24326–24331, Oct. 2013.
[11] M. Ding, P. Wang, and G. Brambilla, “A microfiber coupler tip thermometer,” *Opt. Exp.*, vol. 20, pp. 5402–5408, Feb. 2012.
[12] Y. Chen, S.-C. Yan, X. Zhen, F. Xu, and Y.-Q. Lu, “A miniature reflective micro-force sensor based on a microfiber coupler,” *Opt. Exp.*, vol. 22, pp. 2443–2450, Feb. 2014.
[13] G. Brambilla, V. Finazzi, and D. J. Richardson, “Ultra-low-loss optical fiber nanotapers,” *Opt. Exp.*, vol. 12, pp. 2258–2263, May 2004.
[14] T. Guo *et al.*, “VCSEL-powered and polarization-maintaining fiber-optic grating vector rotation sensor,” *Opt. Exp.*, vol. 21, pp. 19097–19102, Aug. 2013.
[15] J. D. Love and M. Hall, “Polarisation modulation in long couplers,” *Electron. Lett.*, vol. 21, no. 12, pp. 519–521, Jun. 1985.
[16] M. S. Yataki, D. N. Payne, and M. P. Varnham, “All-fibre wavelength filters using concatenated fused-taper couplers,” *Electron. Lett.*, vol. 21, no. 6, pp. 248–249, Mar. 1985.
[17] F. P. Payne, C. D. Hussey, and M. S. Yataki, “Polarisation analysis of strongly fused and weakly fused tapered couplers,” *Electron. Lett.*, vol. 21, pp. 561–563, Jun. 1985.